HHS Public Access

Author manuscript

Glia. Author manuscript; available in PMC 2018 May 01.

Published in final edited form as:

Glia. 2017 May ; 65(5): 804–816. doi:10.1002/glia.23127.

NTE/PNPLA6 is expressed in mature Schwann cells and is required for glial ensheathment of Remak fibers

Janis McFerrin[1], **Bruce L. Patton**[1], **Elizabeth R. Sunderhaus**[1,2], and **Doris Kretzschmar**[1,2]

[1]Oregon Institute of Occupational Health Sciences, Oregon Health & Science University, 3181 SW Sam Jackson Park Road, Portland, OR 97239, USA

[2]Molecular and Medical Genetics, Oregon Health & Science University, 3181 SW Sam Jackson Park Road, Portland, OR 97239, USA

Abstract

Neuropathy Target Esterase (NTE) or patatin-like phospholipase domain containing 6 (PNPLA6) was first linked with a neuropathy occurring after organophosphate poisoning and was later also found to cause complex syndromes when mutated, which can include mental retardation, spastic paraplegia, ataxia, and blindness. NTE/PNPLA6 is widely expressed in neurons but experiments with its *Drosophila* orthologue Swiss-cheese (SWS) suggested that it may also have glial functions. Investigating whether NTE/PNPLA6 is expressed in glia, we found that NTE/PNPLA6 is expressed by Schwann cells in the sciatic nerve of adult mice with the most prominent expression in non-myelinating Schwann cells. Within Schwann cells, NTE/PNPLA6 is enriched at the Schmidt-Lanterman incisures and around the nucleus. When analysing postnatal expression patterns, we did not detect NTE/PNPLA6 in promyelinating Schwann cells, while weak expression was detectable at post-natal day 5 in Schwann cells and increased with their maturation. Interestingly, NTE/PNPLA6 levels were upregulated after nerve crush and localized to ovoids forming along the nerve fibers. Using a GFAP-based knock-out of NTE/PNPLA6, we detected an incomplete ensheathment of Remak fibers whereas myelination did not appear to be affected. These results suggest that NTE/PNPLA6 is involved in the maturation of non-myelinating Schwann cells during development and de-/remyelination after neuronal injury. Since Schwann cells play an important role in maintaining axonal viability and function, it is therefore likely that changes in Schwann cells contribute to the locomotory deficits and neuropathy observed in patients carrying mutations in NTE.

Graphical abstract

Corresponding author: Doris Kretzschmar, Oregon Institute of Occupational Health Sciences, 3181, Oregon Health & Science University, SW Sam Jackson Park Road, Portland, OR 97239, Tel: + 1-503-494-0243; fax: + 1-503-494-6831. kretzsch@ohsu.edu.

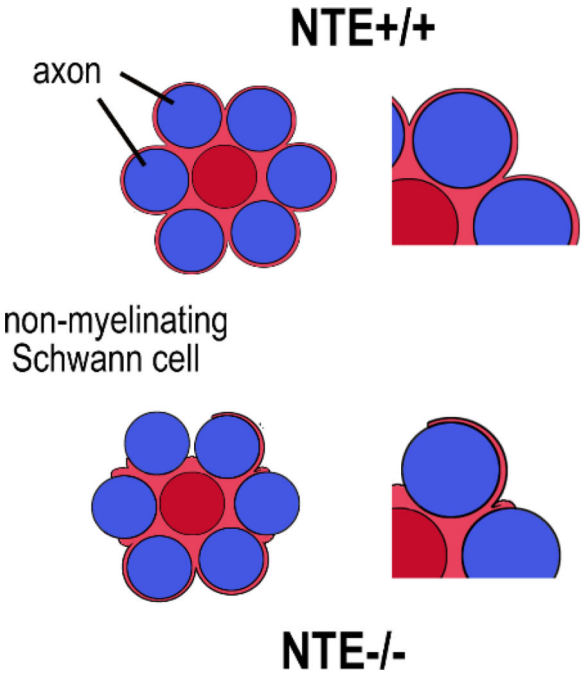

Keywords

non-myelinating Schwann cells; neuropathy; spastic paraplegia; nerve injury; Drosophila SWS

Introduction

Neuropathy Target Esterase (NTE), also called patatin-like phospholipase domain containing 6 (PNPLA6) belongs to a family of phospholipases that are conserved from flies to humans (Lush *et al.*, 1998). Mutations in NTE have been shown to cause a spectrum of diseases that include NTE-related motor neuron disorder or Spastic Paraplegia type 39, a condition that starts in childhood and is characterized by progressive weakness of the upper and lower limbs (Rainier et al. 2008). More recently isolated mutations have been associated with Boucher-Neuhäuser and Gordon-Holmes syndrome, complex disorders that can include hypogonadism, cerebellar atrophy, ataxia, and cognitive impairment (Deik et al. 2014; Synofzik et al. 2014a; Synofzik et al. 2014b; Topaloglu et al. 2014). Furthermore, NTE mutations can lead to Oliver-McFarlane and Laurence-Moon syndrome, which are characterized by retinal degeneration with choroidal atrophy, and in the case of Laurence-Moon syndrome also include progressive spinocerebellar ataxia and spastic paraplegia (Hufnagel et al. 2015; Kmoch et al. 2015). Locomotion problems and ataxia are also observed by environmentally induced changes in NTE activity caused by its interaction with organophosphates that are found in pesticides and nerve gases (Emerick et al. 2012; Glynn 2007; Pope et al. 1993). This phenomenon was first observed in the 1930s, when thousands of people were paralyzed after consuming a beverage (Jamaica Ginger) that contained the organophosphorus compound, tri-ortho-cresyl phosphate (TOCP) (Parascandola 1995). TOCP and other organophosphates bind to and interfere with the phospholipase activity of

NTE, over time leading to a neuropathy that was consequently named Organophosphate-Induced Delayed Neuropathy (OPIDN) (Johnson 1969).

Defects in motor coordination and neuronal degeneration are also detectable after the loss of NTE in the mouse brain (Akassoglou et al. 2004). A complete knock-out of NTE in mice is lethal around day 9 postcoitum with the embryos showing impaired vasculogenesis and placental defects (Moser et al. 2004). The earliest expression of NTE was found in the mesonephric duct followed by expression in the cranial and dorsal root ganglia (Moser et al. 2000). Around day 13 postcoitum, NTE mRNA is also detectable in the spinal ganglia, as well as the epithelium of the respiratory system and the gut. Postnatally, NTE is widely expressed in the brain but becomes more restricted with age, with prominent expression in large neurons in the cortex, olfactory bulb, thalamus, hypothalamus, pons, and medulla oblongata (Glynn et al. 1998; Moser et al. 2000). Similarly, the *Drosophila* ortholog of NTE, Swiss-cheese (SWS), is expressed in most or all neurons in younger animals but becomes more restricted during aging (Muhlig-Versen et al. 2005). SWS shares the highly conserved phospholipase domain with NTE that also contains the organophosphate binding site (Glynn 2013; Muhlig-Versen et al. 2005; Quistad et al. 2003). As in vertebrates, organophosphate treatment of *Drosophila* induces neuronal degeneration and locomotion deficits and similar phenotypes occur in flies carrying mutations in SWS (Kretzschmar et al. 1997; Wentzell et al. 2014). In addition, the functional conservation of NTE and SWS was confirmed by the finding that expression of mouse NTE in *sws* mutant flies can completely restore the wild type phenotype (Muhlig-Versen et al. 2005).

In addition to neurons, SWS was found to be expressed in glia (Muhlig-Versen et al. 2005) and *sws* mutant flies showed defects in glial wrapping of neurons and glial cell death (Kretzschmar et al. 1997). A glial-specific knockdown approach revealed that SWS is required in ensheathing glia in flies (Dutta et al. 2016), a glial subtype that belongs to the neuropil glia which enwraps axons and that has therefore been described to be similar to oligodendrocytes in vertebrates (Freeman and Doherty 2006). In addition, glial-specific SWS knockdown flies showed severe locomotion deficits and changes in synaptic transmission (Dutta et al. 2016), revealing that the loss of SWS in glia impairs neuronal function and contributes to the behavioural phenotypes of the *sws* mutant. Although glial expression of NTE has not previously been described in vertebrates, NTE-activity has been detected in both mammalian neurons and glial cells (Glynn 2006; Glynn 2007). Furthermore, the glial phenotype in *sws* mutants and knockdown flies can also be rescued by the expression of mouse NTE (Dutta et al. 2015; Muhlig-Versen et al. 2005), further indicating that this protein family may serve evolutionarily conserved functions in glial cells. Here we demonstrate that NTE is expressed in Schwann cells within the sciatic nerves of mice, particularly in non-myelinating Schwann cells, and that its loss induces defects in the glial wrapping of Remak fibers.

Materials and Methods

Animals

Mice were maintained and handled according to the guidelines established by the National Institutes of Health and approved by the Oregon Health and Science University's

Institutional Animal Care and Use Committee. All mice were housed in PIV caging on a 12/12-hour light/dark cycle, and provided with food and water ad libidum. C57BL/6J mice were used as wild type mice. NTEflox/flox mice were previously described by (Akassoglou et al. 2004) and kindly provided by M. Chao, Skirball Institute, New York University School of Medicine. Mice carrying Tamoxifen (TAM)-inducible GFAP-cre carrying mice were kindly provided by our colleague G. Mandel (Vollum Institute, OHSU) and are described in (Lioy et al. 2011). Both lines were backcrossed five generations to C57BL/6J before crossing them to obtain heterozygous Tam-GFAP-cre; NTEflox mice, which were then crossed with each other. The genotypes of the progeny were identified by PCR analyses of tail-tip DNA, using the following sense (-*S*) and antisense (-*AS*) primers: GFAP-cre-*S*: 5′-CCTGGAAAATGCTTCTGTCCG -3′; -*AS*: 5′-CAGGGTGTTATAAGCAATCCC -3′. *NTE-S*: 5′-GCTTAAGGGCACCTGCCAGC -3′; -*AS*: 5′-GGTCTTGTAGCCTGCAGTCC -3′. PCR was performed with an annealing temperature of 50°C with 35 cycle. Axonal injury was induced by repeated crushes of one sciatic nerve with foreceps using anesthetized 4-6 week-old mice as described in (Patton et al. 1999) while the unijured nerve was used as a matched control.

Schwann cell cultures

Primary Schwann cell cultures were established from the sciatic nerves of neonatal C57BL/6J mice as described in (Sherman et al. 2000). Cells were initially grown on poly-l-lysine–coated tissue culture plastic (Sigma-Aldrich) in DMEM supplemented with 10% FBS, 5 ng/ml recombinant human (rh)-GGF2, and 2 μM forskolin (Calbiochem-Novabiochem), and then switched to a serum-free defined medium (N2) for an additional 24 h.

Histology

For resin sections, animals were sacrificed and perfused with 3% (wt/vol) paraformaldehyde (PFA), 1% (vol/vol) glutaraldehyde, in PBS. Disected nerves were then incubated overnight at 4°C in 4% PFA, 4% glutaraldehyde in 0.1 M cacodylate and 1-mm pieces were post-fixed 1 h in 1% OsO_4, dehydrated through ethanol, and embedded in Epon. Semithin sections (1 μm) were stained with toluidine blue (1% in alcohol) and imaged by digital color photomicroscopy. Ultrathin sections (50 nm) were stained with uranyl acetate and analyzed using an FEI Tecnai G^2 transmission electron microscope.

Immunohistochemistry

Immunohistochemistry was performed as described in (Miner et al. 1997), using 8–10-μm cryostat sections cut from OCT-embedded unfixed tissue that had been snap frozen in 2-methylbutane at −150°C. Sections were fixed for 20 min in 2% PFA, incubated with 100 mM glycine in PBS for 10 min and blocked in PBS with 5% BSA and 0.5% Triton X-100. Primary antibodies were diluted in PBS containing 5% (wt/vol) BSA and applied overnight. Anti-peripherin (8G2) was obtained from Sigma and was used at 1:1000, anti-GFAP (AB5541) from EMD Millipore and was used at 1:500, anti-L1 from the Developmental Studies Hybridoma Bank (created by the NICHD of the NIH and maintained at The University of Iowa, Department of Biology, Iowa City) and was used at 1:200, anti-MAG from Santa Cruz Biotechnology (A11) and was used at 1:200, and anti-CD44 (5GA) was

kindly provided by L. Sherman (OHSU) and used at 1:200 (Sleeman et al. 1996) and anti-MBP (EMD Millipore) was provided by F. Robinson (OHSU), and was used at 1:200. Rhodamine-Phalloidin was obtained from Thermo Fisher Scientific. A rabbit antiserum against NTE (Chang et al. 2005) was kindly provided by Y.J. Wu (Chinese Academy of Science, Bejing, China) and used at 1:500, while anti-NTE from Abcam (ab110391) was used at 1:200. Bound antibodies were then detected with the following species-specific fluorescent-labeled secondary antibodies (1 h incubation, used at 1:1000): FITC-conjugated anti-mouse (Boehringer Mannheim), FITC-conjugated anti-rat (EMD Millipore), and Cy3-conjugated anti-rabbit (Molecular Probes, Thermoscientific). DAPI (Sigma) was used to visualize nuclei.

Analyzing myelination and glial wrapping of Remak fibers

The g-ratio was determined on photographs of semithin sections stained with tolouidin blue as a means of measuring myelin thickness. Quantification of the ensheathment of Remak fibers was performed on electron microscopic sections by determining the percentage of fibers that were not completely wrapped by glial sheaths in each Remak bundle. Statistics were conducted using GraphPad Prism and Student's t-tests.

Results

NTE is expressed in Schwann cells

Mutations in NTE cause a variety of symptoms, whereby locomotion deficits are the most common phenotype. Similarly, the delayed neuropathy caused by the inhibition of NTE by organophosphates is also characterized by movement problems, especially affecting the lower limbs. We therefore investigated whether NTE might play a role in the peripheral nervous system, particularly in Schwann cells, focusing on the sciatic nerve. Using an anti-NTE antisera kindly provided by Y-J. Wu (Chinese Academy of Science), we could readily detect NTE in immunolabeled frozen sections of sciatic nerves prepared from adult mice at post-natal day (PND) 42 (Fig. 1A, arrowheads). Notably, some of the immunostaining was detectable in close proximity to DAPI-positive nuclei (Fig. 1B), suggesting its expression in glial cell bodies. A similar pattern was also seen when using a commercially available anti-NTE (data not shown). To verify this observation, we co-immunolabeled the sections with anti-GFAP, which is highly expressed by astrocytes in the CNS but is also expressed by non-myelinating and immature Schwann cells within the peripheral nervous system (Jessen and Mirsky 2005; Jessen et al. 1990). Although some cells were only positive for NTE (arrow in Fig. 1B), many of the NTE staining co-localized with this glial marker (arrowheads, Fig. 1A', B"). Since these sections were derived from adult animals, this pattern of immunoreactivity suggests that NTE is abundantly expressed by non-myelinating Schwann cells.

To verify this observation, we also co-immunolabeled sciatic nerve sections with anti-CD44 and antiperipherin. Whereas anti-peripherin is a marker for unmyelinated axons (Lariviere et al. 2002; Yuan et al. 2012), anti-CD44 labels non-myelinating Schwann cells in the adult sciatic nerve (Gorlewicz et al. 2009; Sherman et al. 2000). As shown in figure 2 NTE was detected in close proximity to peripherin (arrowheads, 2A-A") and co-localized with CD44

(Fig. 2B-B"). The co-localization of NTE with CD44 was even more apparent at higher magnification (Fig. 2E, E' shows the cell indicated by the arrow in 2B). By analyzing sections from the tibial nerve, we again detected prominent expression of NTE in non-myelinating Schwann cells (white arrows, Fig. 2C) and weaker expression in the cytoplasm of myelinating Schwann cells, detectable as discontinuous rings (red arrowheads, Fig. 2C). Consistent with previous reports of NTE expression in neurons, we also found weak expression in axons (red arrows, Fig. 2C). Lastly, we confirmed the expression of NTE in Schwann cells by performing immunohistochemistry with anti-NTE antibodies on cultured primary Schwann cells (Fig. 2D).

NTE is enriched at Schmidt-Lanterman incisures

Schwann cells form distinct compartments along the axon, including the nodes of Ranvier, Cajal bands, and Schmidt-Lanterman incisures (Ghabriel and Allt 1979; Ghabriel and Allt 1980; Salzer 2003; Salzer et al. 2008; Ushiki and Ide 1987). To determine whether NTE is localized to any of these compartments, we prepared teased fibers from adult (PND42) sciatic nerves. Cajal bands and Schmidt-Lanterman incisures (SLIs) are cytoplasmic channels that are actin-rich (Gupta et al. 2012; Jung et al. 2011; Salzer 2003) and can therefore be stained with Phalloidin. As shown in figure 3, NTE co-localized with Phalloidin in SLIs (arrowheads, Fig. 3A, A', B, B') and it could be found in close proximity to nuclei (arrows, Fig. 3B, B"), consistent with findings in neurons that NTE localizes to the endoplasmic reticulum (Li et al. 2003). At higher magnification, weaker NTE staining could also be detected in Cajal bands (figure 3C, arrows). As described below (see Fig. 7A), we subsequently confirmed the enrichment of NTE in SLIs by co-labelling with another marker for this compartment, myelin-associated glycoprotein (MAG) (Trapp 1990).

NTE is not expressed in immature or promyelinating Schwann cells

Schwann cell precursors are produced from the neural crest and develop into immature Schwann cells during embryonic development, surrounding bundles of closely associated axons (Jessen and Mirsky 1997; Jessen and Mirsky 2005; Monk et al. 2015; Woodhoo and Sommer 2008). Radial sorting of axons occurs around birth, whereby large diameter axons are separated by Schwann cells that differentiate and form myelin. The remaining small caliber axons are ensheathed in small groups by the differentiating non-myelinating Schwann cells, thereby forming the Remak bundles, a process that is completed around PND10. To investigate whether the expression of NTE is developmentally regulated and correlates with the differentiation of Schwann cells, we immunohistochemically stained sciatic nerve sections derived from different postnatal stages with anti-NTE. Sections were also co-stained with anti-L1, a cell adhesion molecule expressed in Schwann cell precursors, immature Schwann cells, and mature non-myelinating Schwann cells (Mirsky and Jessen 2009; Stewart et al. 1995). As shown in figure 4A, NTE was absent from early postnatal nerves (PND0), whereas weak immunopositive staining was detectable at PND5 (Fig. 4B, B'). At PND10, NTE was readily detectable in L1-positive cells (Fig. 4C, C'), correlating with the presence of mature non-myelinating Schwann cells. However, its levels were still lower than observed in the adult sciatic nerve. A similar result was obtained when co-staining sciatic nerves from PND0, PND5 and PND8 with peripherin (Supp. Fig. 1). Although the onset of NTE staining around PND5 suggested that it is not expressed in

immature or promyelinating Schwann cells, we addressed this further by using antibodies against MAG and myelin basic protein (MBP), whose expression starts in the promyelination stage (Martini and Schachner 1986; Martini and Schachner 1997; Schachner and Bartsch 2000). As expected, both MAG and MBP were detectable at PND3, but we did not observe any NTE staining at this age (Fig. 5A, Supp. Fig. 2A). Confirming our earlier studies, weak NTE expression was detectable at PND5 (Fig. 5B) and increased levels were detected at PND14, at which stage much of the NTE staining co-localized with MAG and MBP (Fig. 5C, Supp. Fig. 2B, C). These results confirms that NTE is not expressed in promyelinating Schwann cells but that it is expressed later during the maturation of myelinating and non-myelinating Schwann cells.

NTE is upregulated after peripheral nerve injury

Many proteins expressed during the development of Schwann cells (including L1, peripherin, and GFAP), are also induced after neuronal injury and axonal re-growth of peripheral nerves, a process that requires the de-differentiation and proliferation of Schwann cells (Berg et al. 2013; Jessen et al. 1990; Martini 1994; Neuberger and Cornbrooks 1989; Triolo et al. 2006). In addition, it has been shown that the SLIs play an important role in demyelination after injury and during Wallerian degeneration, due the fragmentation of myelin occurring adjacent to SLIs (Berger and Gupta 2006; Ghabriel and Allt 1979; Jung et al. 2011; Klein et al. 2014). We therefore investigated whether we could detect changes in the levels or localization of NTE after injury. Performing immunohistochemistry on sciatic nerves of adult mice harvested four days after unilateral crush lesions indeed revealed an upregulation of NTE as well as GFAP (Fig. 6A), compared to their expression levels in matched uninjured nerves (Fig. 6C). Eleven days after the injury, the levels of NTE begin to decrease, coinciding with the decrease in GFAP levels (Fig. 6E). Similarly, we detected an upregulation of NTE four days after injury in Western blots (Supp. Fig. 3). Our immunohistochemical analysis also revealed a prominent ring-shaped pattern of staining (arrowheads in Fig. 6A, B), which though weaker, could still be detected after eleven days (Fig. 6E, F). To determine whether this pattern could be due to an upregulation of NTE in the SLIs, we again used teased fiber preparations from nerves obtained four days after crush. As noted above, we found that NTE was enriched in Schmidt-Lanterman incisures in uninjured control fibers, where it colocalized with MAG (Fig. 7A). In contrast, NTE expression was widespread along the damaged fibers, localizing to ovoids (arrowheads, Fig. 7B). Co-staining these preparations with MAG suggested that most of the NTE staining does not co-localize with MAG (arrows, Fig. 7B). At a higher magnification, we could detect MAG staining adjacent to both sides of weakly stained NTE-positive ovoids (Fig. 7C, green arrows). In the case of the ovoid with higher NTE expression levels, NTE and MAG co-localized at the margins of the ovoid (Fig. 7C, white arrows), whereas MAG is absent in the case of the ovoid with the highest NTE expression levels (Fig. 7C, arrowhead). Together, these results reveal that NTE changes it subcellular localization after injury and shows a dynamic co-localization pattern with MAG.

The conditional glial knock-out of NTE results in incomplete wrapping of Remak fibers

The expression of NTE during early postnatal stages and its induction after nerve injury suggest that NTE may play a role in the maturation of Schwann cells. As mentioned above, a

complete knock-out of NTE is lethal during embryonic development (Moser et al. 2004), while a nestin-cre mediated conditional knock-out of NTE has been shown to result in neuronal degeneration in the CNS (Akassoglou et al. 2004). To specifically assess the glial function of NTE, we crossed Tamoxifen (TAM)-inducible GFAP-cre carrying mice (Lioy et al. 2011) with NTE-flox mice (Akassoglou et al. 2004). Due to GFAP being expressed in non-myelinating and immature Schwann cells (Jessen and Mirsky 2005; Jessen et al. 1990) and our evidence that NTE co-localizes with GFAP in Schwann cells (Fig. 1), this strategy should specifically delete NTE in peripheral glia. GFAP-cre was induced by daily neonatal administration of TAM through maternal lactation starting at PND0 for three weeks. Performing sciatic nerve sections at PND14 from the conditional knock-out animals revealed a strong downregulation of NTE levels in the NTE(fl/fl);Cre+ mice (Fig. 8B, D) when compared to their TAM-treated NTE(+/+);Cre+ siblings (Fig. 8A, C). As expected, the levels of GFAP (Fig. 8A, B) and CD44 (Fig. 8C, D) were not altered in the conditional NTE knock-out.

Next we analyzed sciatic nerve sections from four-month-old conditional knock-out mice at the light and electron microscopic level to determine whether these mice show defects in myelination or Remak bundle formation. A comparison of toloudine-blue-stained sections from TAM-treated NTE(fl/fl);Cre+ mice (Fig. 9A) with treated NTE(+/+);Cre+ siblings (Fig. 9B) did not reveal defects in myelination, nor was the g-ratio significantly different (Fig. 9C). Furthermore, we did not detect defects in myelination in electron microscopic images (data not shown). Together, this result suggests that the conditional knock-out of NTE had no consequences for the differentiation of myelinating Schwann cells. In contrast, we did observe effects on non-myelinating Schwann cells in our electron microscopic studies. Whereas the Remak fibers in four month old control mice (TAM treated NTE(+/+);Cre+ siblings) were almost always completely ensheathed by non-myelinating Schwann cells (Fig. 10A, C), many of these fibers were incompletely wrapped in TAM-treated NTE(fl/fl);Cre+ animals (arrowheads, Fig. 10B, D). In addition, some of the axons in the conditional knock-out animals looked shrunken and more electron dense, indicating that these fibers were undergoing degeneration (arrows, Fig. 10B, D). Quantifying this glial wrapping phenotype by determining the percentage of incompletely wrapped axons in a Remak bundle, we found that on average, 12% of axons showed mostly small gaps in their glial sheaths in NTE(+/+), whereas this number increased to 55% in the conditional knock-out animals (Fig. 10E). This result shows that the loss of NTE does affect the maturation of non-myelinating Schwann cells and the formation of Remak bundles, corresponding to the higher expression levels of NTE in this Schwann cell population.

DISCUSSION

NTE was previously shown to be expressed in neurons (Glynn et al. 1998; Moser et al. 2000), but experiments with cultured astrocytes suggested that its activity is also present in glia (Glynn 2007; Glynn 2012). A role for NTE in glia was also suggested from studies in *Drosophila*, which demonstrated the presence of SWS (the fly orthologue of NTE) in CNS glia and showed that expression of mouse NTE in *Drosophila* glia could rescue the glial defects seen in *sws* mutant flies (Muhlig-Versen et al. 2005). Focusing on the sciatic nerve, we verified that NTE is present in axons, but we could also detect its expression in Schwann

cells. The levels of NTE were highest in non-myelinated Schwann cells, although lower levels could be detected in myelinating Schwann cells, with an enrichment at Schmidt-Lanterman incisures and around the nucleus. The latter observation is in agreement with the localization of NTE to the endoplasmic reticulum, as has been described in neurons (Li et al. 2003; Zaccheo et al. 2004). Furthermore, NTE expression was detectable in primary Schwann cell cultures lacking neurons.

By analyzing the developmental profile of NTE expression, we found that it was absent during early postnatal stages of Schwann cell differentiation. Around birth, the peripheral nerves go through a stage of axonal sorting, in which immature Schwann cells either associate with large axons and differentiate into mature myelinating Schwann cells or with the small Remak fibers, which are enwrapped by Schwann cells but are not myelinated (Feltri et al. 2015; Kaplan et al. 2009). This process requires a close interaction between neurons and Schwann cells and is regulated by several signaling pathways, including axonal signaling via Neuregulin 1 and ErbB receptors, as well as extracellular matrix signaling via laminin and β1 integrin and dystroglycan receptors (Berti et al. 2011; Birchmeier and Nave 2008; Monk et al. 2015; Nave and Salzer 2006; Newbern and Birchmeier 2010; Taveggia et al. 2005; Woodhoo and Sommer 2008). After this sorting phase, the Schwann cells differentiate into mature cells that form myelin sheaths (around large axons) or enwrap Remak fibers, which also requires signaling between the axons and glial populations (Fricker et al. 2009; Raphael et al. 2011; Yu et al. 2009). NTE was not detectable at PND0 and its levels were still quite low at PND5, suggesting that it is not expressed in immature or promyelinating Schwann cells. This was confirmed by co-immunolabeling with anti-MAG and anti BMP. In contrast, NTE levels increased a few days after birth (PND8), suggesting a role late in Schwann cell maturation. When we examined GFAP-Cre mediated conditional NTE knock-out animals, we could not detect effects on axonal sorting or myelination, indicating that NTE is not required for the differentiation of myelinating Schwann cells. However, we did find that non-myelinating Schwann cells failed to completely enwrap Remak fibers, which correlated with the higher expression levels in these cells, showing that NTE is required for the maturation of non-myelinating Schwann cells.

Inhibition of NTE by organophosphates induces a neuropathy that shows the characteristic signs of Wallerian degeneration (Abou-Donia 2003; Dyer et al. 1992; Emerick et al. 2012). We therefore also investigated whether we could detect changes in NTE after neuronal injury caused by nerve crush. Indeed, we found not only an increase in NTE levels following injury but also a strong accumulation of NTE in ovoids distributed along the fibers. Surprisingly, it appeared that NTE was excluded from the SLIs after injury, although it was enriched in SLIs in uninjured fibers and SLIs have been shown to play an important role in demyelination responses after injury or disease (Jung et al. 2011; Klein et al. 2014). During Wallerian degeneration, the myelin sheath becomes fragmented and forms ovoids similar to the ones we observed with NTE immunolabeling, a process that occurs near the SLIs (Ghabriel and Allt 1979; Jung et al. 2011). The similarity of the NTE-positive ovoids with the ovoids observed during myelin fragmentation indicates that NTE may play a role in demyelination responses after injury. NTE is a phospholipase that hydrolyzes phosphatidylcholine and lysophosphatidylcholine (LPC) by degrading it to glycerophosphocholine (Quistad et al. 2003; van Tienhoven et al. 2002). Of note is that LPC

synthesis is also upregulated after injury and is a well-known demyelinating agent (Ghasemlou et al. 2007; Velasco et al. 2016). It is therefore possible that NTE plays a role in the changes that occur in Schwann cell membranes during demyelination and/or remyelination.

Problems with motor coordination and paralysis are prominent symptoms of NTE-related diseases. Likewise a nestin-Cre induced NTE knock-out resulted in hindlimb dysfunction and behavioral deficits in Rotarod tests (Akassoglou et al. 2004; Read et al. 2009). However, due to Nestin being expressed in the early development of the peripheral and central nervous system (Michalczyk and Ziman 2005), these experiments did not distinguish the roles of NTE in the CNS versus the PNS, nor did they discriminate between its potential functions in glia versus neurons. Although the loss of neuronal NTE most likely contributes to disease progression, the maintenance of axonal viability is strongly dependent on their associated glial cell partners, and defects in Schwann cells have been shown to cause peripheral neuropathies like Charcot-Marie-Tooth (Berger et al. 2006). In addition, our previous studies in *Drosophila* showed that a glial-specific knockdown not only caused incomplete glial wrapping of axons but also induced severe locomotion defects and changes in neuronal function (Dutta et al. 2015), suggesting that glial loss of NTE contributes to the pathogenesis of NTE-related diseases. Lastly, given the role of disrupted Remak bundles in neuropathic pain (Koltzenburg and Scadding 2001), the defects in Remak bundle formation that we detected in the conditional knock-out mice indicates that NTE could also play a role in the neuropathic pain responses that can accompany peripheral neuropathies.

Supplementary Material

Refer to Web version on PubMed Central for supplementary material.

Acknowledgments

Thanks are due to the OHSU imaging facility, which was supported by the NIH P30NS061800 grant and provided support for the electron microscopic studies. We are also grateful for valuable input from Fred Robinson and Charles Allen, both OHSU. This work was supported by a grant (NS047663) to D.K. from the National Institute of Health.

References

Abou-Donia MB. Organophosphorus ester-induced chronic neurotoxicity. Arch Environ Health. 2003; 58(8):484–497. [PubMed: 15259428]

Akassoglou K, Malester B, Xu J, Tessarollo L, Rosenbluth J, Chao MV. Brain-specific deletion of neuropathy target esterase/swisscheese results in neurodegeneration. Proc Natl Acad Sci U S A. 2004; 101(14):5075–5080. [PubMed: 15051870]

Berg A, Zelano J, Pekna M, Wilhelmsson U, Pekny M, Cullheim S. Axonal regeneration after sciatic nerve lesion is delayed but complete in GFAP- and vimentin-deficient mice. PLoS One. 2013; 8(11):e79395. [PubMed: 24223940]

Berger BL, Gupta R. Demyelination secondary to chronic nerve compression injury alters Schmidt-Lanterman incisures. J Anat. 2006; 209(1):111–118. [PubMed: 16822274]

Berger P, Niemann A, Suter U. Schwann cells and the pathogenesis of inherited motor and sensory neuropathies (Charcot-Marie-Tooth disease). Glia. 2006; 54(4):243–257. [PubMed: 16856148]

Berti C, Bartesaghi L, Ghidinelli M, Zambroni D, Figlia G, Chen ZL, Quattrini A, Wrabetz L, Feltri ML. Non-redundant function of dystroglycan and beta1 integrins in radial sorting of axons. Development. 2011; 138(18):4025–4037. [PubMed: 21862561]

Birchmeier C, Nave KA. Neuregulin-1, a key axonal signal that drives Schwann cell growth and differentiation. Glia. 2008; 56(14):1491–1497. [PubMed: 18803318]

Chang P-A, Chen R, Wu Y-J. Reduction of neuropathy target esterase does not affect neuronal differentiation, but moderate expression induces neuronal differentiation in human neuroblastoma (SK-N-SH) cell line. Molecular Brain Research. 2005; 141(1):30–38. [PubMed: 16122834]

Deik A, Johannes B, Rucker JC, Sanchez E, Brodie SE, Deegan E, Landy K, Kajiwara Y, Scelsa S, Saunders-Pullman R, et al. Compound heterozygous PNPLA6 mutations cause Boucher-Neuhauser syndrome with late-onset ataxia. J Neurol. 2014; 261(12):2411–2423. [PubMed: 25267340]

Dutta S, Rieche F, Eckl N, Duch C, Kretzschmar D. Glial expression of Swiss-cheese (SWS), the Drosophila orthologue of Neuropathy Target Esterase, is required for neuronal ensheathment and function. Dis Model Mech. 2015

Dutta S, Rieche F, Eckl N, Duch C, Kretzschmar D. Glial expression of Swiss cheese (SWS), the Drosophila orthologue of neuropathy target esterase (NTE), is required for neuronal ensheathment and function. Dis Model Mech. 2016; 9(3):283–294. [PubMed: 26634819]

Dyer KR, Jortner BS, Shell LG, Ehrich M. Comparative dose-response studies of organophosphorus ester-induced delayed neuropathy in rats and hens administered mipafox. Neurotoxicology. 1992; 13(4):745–755. [PubMed: 1302301]

Emerick GL, DeOliveira GH, dos Santos AC, Ehrich M. Mechanisms for consideration for intervention in the development of organophosphorus-induced delayed neuropathy. Chem Biol Interact. 2012; 199(3):177–184. [PubMed: 22819951]

Feltri ML, Poitelon Y, Previtali SC. How Schwann Cells Sort Axons: New Concepts. Neuroscientist. 2015

Freeman MR, Doherty J. Glial cell biology in Drosophila and vertebrates. Trends Neurosci. 2006; 29(2):82–90. [PubMed: 16377000]

Fricker FR, Zhu N, Tsantoulas C, Abrahamsen B, Nassar MA, Thakur M, Garratt AN, Birchmeier C, McMahon SB, Wood JN, et al. Sensory axon-derived neuregulin-1 is required for axoglial signaling and normal sensory function but not for long-term axon maintenance. J Neurosci. 2009; 29(24):7667–7678. [PubMed: 19535578]

Ghabriel MN, Allt G. The role of Schmidt-Lanterman incisures in Wallerian degeneration. Acta Neuropathologica. 1979; 48(2):83–93.

Ghabriel MN, Allt G. Schmidt-Lanterman IncisuresIA quantitative teased fibre study of remyelinating peripheral nerve fibres. Acta Neuropathol. 1980; 52(2):85–95. [PubMed: 7435168]

Ghasemlou N, Jeong SY, Lacroix S, David S. T cells contribute to lysophosphatidylcholine-induced macrophage activation and demyelination in the CNS. Glia. 2007; 55(3):294–302. [PubMed: 17096403]

Glynn P. A mechanism for organophosphate-induced delayed neuropathy. Toxicol Lett. 2006; 162(1): 94–97. [PubMed: 16309859]

Glynn P. Axonal degeneration and neuropathy target esterase. Arh Hig Rada Toksikol. 2007; 58(3): 355–358. [PubMed: 18050888]

Glynn P. Neuronal phospholipid deacylation is essential for axonal and synaptic integrity. Biochim Biophys Acta. 2012

Glynn P. Neuronal phospholipid deacylation is essential for axonal and synaptic integrity. Biochim Biophys Acta. 2013; 1831(3):633–641. [PubMed: 22903185]

Glynn P, Holton JL, Nolan CC, Read DJ, Brown L, Hubbard A, Cavanagh JB. Neuropathy target esterase: immunolocalization to neuronal cell bodies and axons. Neuroscience. 1998; 83(1):295–302. [PubMed: 9466418]

Gorlewicz A, Wlodarczyk J, Wilczek E, Gawlak M, Cabaj A, Majczynski H, Nestorowicz K, Herbik MA, Grieb P, Slawinska U, et al. CD44 is expressed in non-myelinating Schwann cells of the adult rat, and may play a role in neurodegeneration-induced glial plasticity at the neuromuscular junction. Neurobiology of Disease. 2009; 34(2):245–258. [PubMed: 19385056]

Gupta R, Nassiri N, Hazel A, Bathen M, Mozaffar T. Chronic nerve compression alters Schwann cell myelin architecture in a murine model. Muscle & nerve. 2012; 45(2):231–241. [PubMed: 22246880]

Hufnagel RB, Arno G, Hein ND, Hersheson J, Prasad M, Anderson Y, Krueger LA, Gregory LC, Stoetzel C, Jaworek TJ, et al. Neuropathy target esterase impairments cause Oliver-McFarlane and Laurence-Moon syndromes. J Med Genet. 2015; 52(2):85–94. [PubMed: 25480986]

Jessen KR, Mirsky R. Embryonic Schwann cell development: the biology of Schwann cell precursors and early Schwann cells. Journal of Anatomy. 1997; 191(Pt 4):501–505. [PubMed: 9449069]

Jessen KR, Mirsky R. The origin and development of glial cells in peripheral nerves. Nat Rev Neurosci. 2005; 6(9):671–682. [PubMed: 16136171]

Jessen KR, Morgan L, Stewart HJ, Mirsky R. Three markers of adult non-myelin-forming Schwann cells, 217c(Ran-1), A5E3 and GFAP: development and regulation by neuron-Schwann cell interactions. Development. 1990; 109(1):91–103. [PubMed: 2209471]

Johnson MK. The delayed neurotoxic effect of some organophosphorus compounds: identification of the phosphorylation site as an esterase. T Biochem J. 1969; 114:711–714.

Jung J, Cai W, Lee HK, Pellegatta M, Shin YK, Jang SY, Suh DJ, Wrabetz L, Feltri ML, Park HT. Actin polymerization is essential for myelin sheath fragmentation during Wallerian degeneration. The Journal of neuroscience : the official journal of the Society for Neuroscience. 2011; 31(6): 2009–2015. [PubMed: 21307239]

Kaplan S, Odaci E, Unal B, Sahin B, Fornaro M. Chapter 2: Development of the peripheral nerve. Int Rev Neurobiol. 2009; 87:9–26. [PubMed: 19682631]

Klein D, Groh J, Wettmarshausen J, Martini R. Nonuniform molecular features of myelinating Schwann cells in models for CMT1: Distinct disease patterns are associated with NCAM and c-Jun upregulation. Glia. 2014; 62(5):736–750. [PubMed: 24526449]

Kmoch S, Majewski J, Ramamurthy V, Cao S, Fahiminiya S, Ren H, MacDonald IM, Lopez I, Sun V, Keser V, et al. Mutations in PNPLA6 are linked to photoreceptor degeneration and various forms of childhood blindness. Nat Commun. 2015; 6:5614. [PubMed: 25574898]

Koltzenburg M, Scadding J. Neuropathic pain. Curr Opin Neurol. 2001; 14(5):641–647. [PubMed: 11562577]

Kretzschmar D, Hasan G, Sharma S, Heisenberg M, Benzer S. The swiss cheese mutant causes glial hyperwrapping and brain degeneration in Drosophila. J Neurosci. 1997; 17(19):7425–7432. [PubMed: 9295388]

Lariviere RC, Nguyen MD, Ribeiro-da-Silva A, Julien JP. Reduced number of unmyelinated sensory axons in peripherin null mice. J Neurochem. 2002; 81(3):525–532. [PubMed: 12065660]

Li Y, Dinsdale D, Glynn P. Protein domains, catalytic activity, and subcellular distribution of neuropathy target esterase in Mammalian cells. J Biol Chem. 2003; 278(10):8820–8825. [PubMed: 12514188]

Lioy DT, Garg SK, Monaghan CE, Raber J, Foust KD, Kaspar BK, Hirrlinger PG, Kirchhoff F, Bissonnette JM, Ballas N, et al. A role for glia in the progression of Rett's syndrome. Nature. 2011; 475(7357):497–500. [PubMed: 21716289]

Martini R. Expression and functional roles of neural cell surface molecules and extracellular matrix components during development and regeneration of peripheral nerves. J Neurocytol. 1994; 23(1): 1–28. [PubMed: 8176415]

Martini R, Schachner M. Immunoelectron microscopic localization of neural cell adhesion molecules (L1, N-CAM, and MAG) and their shared carbohydrate epitope and myelin basic protein in developing sciatic nerve. J Cell Biol. 1986; 103(6 Pt 1):2439–2448. [PubMed: 2430983]

Martini R, Schachner M. Molecular bases of myelin formation as revealed by investigations on mice deficient in glial cell surface molecules. Glia. 1997; 19(4):298–310. [PubMed: 9097074]

Michalczyk K, Ziman M. Nestin structure and predicted function in cellular cytoskeletal organisation. Histol Histopathol. 2005; 20(2):665–671. [PubMed: 15736068]

Miner JH, Patton BL, Lentz SI, Gilbert DJ, Snider WD, Jenkins NA, Copeland NG, Sanes JR. The Laminin α Chains: Expression, Developmental Transitions, and Chromosomal Locations of α1-5, Identification of Heterotrimeric Laminins 8-11, and Cloning of a Novel α3 Isoform. The Journal of Cell Biology. 1997; 137(3):685–701. [PubMed: 9151674]

Mirsky, R., Jessen, KR. Schwann Cell Development A2 - Squire, Larry R. Encyclopedia of Neuroscience. Oxford: Academic Press; 2009. p. 463-473.

Monk KR, Feltri ML, Taveggia C. New insights on Schwann cell development. Glia. 2015; 63(8): 1376–1393. [PubMed: 25921593]

Moser M, Li Y, Vaupel K, Kretzschmar D, Kluge R, Glynn P, Buettner R. Placental failure and impaired vasculogenesis result in embryonic lethality for neuropathy target esterase-deficient mice. Mol Cell Biol. 2004; 24(4):1667–1679. [PubMed: 14749382]

Moser M, Stempfl T, Li Y, Glynn P, Buttner R, Kretzschmar D. Cloning and expression of the murine sws/NTE gene. Mech Dev. 2000; 90(2):279–282. [PubMed: 10640712]

Muhlig-Versen M, da Cruz AB, Tschape JA, Moser M, Buttner R, Athenstaedt K, Glynn P, Kretzschmar D. Loss of Swiss cheese/neuropathy target esterase activity causes disruption of phosphatidylcholine homeostasis and neuronal and glial death in adult Drosophila. J Neurosci. 2005; 25(11):2865–2873. [PubMed: 15772346]

Nave KA, Salzer JL. Axonal regulation of myelination by neuregulin 1. Curr Opin Neurobiol. 2006; 16(5):492–500. [PubMed: 16962312]

Neuberger TJ, Cornbrooks CJ. Transient modulation of Schwann cell antigens after peripheral nerve transection and subsequent regeneration. J Neurocytol. 1989; 18(5):695–710. [PubMed: 2515258]

Newbern J, Birchmeier C. Nrg1/ErbB signaling networks in Schwann cell development and myelination. Semin Cell Dev Biol. 2010; 21(9):922–928. [PubMed: 20832498]

Parascandola J. The Public Health Service and Jamaica ginger paralysis in the 1930s. Public Health Reports. 1995; 110(3):361–363. [PubMed: 7610232]

Patton BL, Connoll AM, Martin PT, Cunningham JM, Mehta S, Pestronk A, Miner JH, Sanes JR. Distribution of ten laminin chains in dystrophic and regenerating muscles. Neuromuscul Disord. 1999; 9(6-7):423–33. [PubMed: 10545049]

Pope CN, Tanaka D Jr, Padilla S. The role of neurotoxic esterase (NTE) in the prevention and potentiation of organophosphorus-induced delayed neurotoxicity (OPIDN). Chem Biol Interact. 1993; 87(1-3):395–406. [PubMed: 8343996]

Quistad GB, Barlow C, Winrow CJ, Sparks SE, Casida JE. Evidence that mouse brain neuropathy target esterase is a lysophospholipase. Proc Natl Acad Sci U S A. 2003; 100(13):7983–7987. [PubMed: 12805562]

Rainier S, Bui M, Mark E, Thomas D, Tokarz D, Ming L, Delaney C, Richardson RJ, Albers JW, Matsunami N, et al. Neuropathy target esterase gene mutations cause motor neuron disease. Am J Hum Genet. 2008; 82(3):780–785. [PubMed: 18313024]

Raphael AR, Lyons DA, Talbot WS. ErbB signaling has a role in radial sorting independent of Schwann cell number. Glia. 2011; 59(7):1047–1055. [PubMed: 21491500]

Read DJ, Li Y, Chao MV, Cavanagh JB, Glynn P. Neuropathy target esterase is required for adult vertebrate axon maintenance. J Neurosci. 2009; 29(37):11594–11600. [PubMed: 19759306]

Salzer JL. Polarized domains of myelinated axons. Neuron. 2003; 40(2):297–318. [PubMed: 14556710]

Salzer JL, Brophy PJ, Peles E. Molecular domains of myelinated axons in the peripheral nervous system. Glia. 2008; 56(14):1532–1540. [PubMed: 18803321]

Schachner M, Bartsch U. Multiple functions of the myelin-associated glycoprotein MAG (siglec-4a) in formation and maintenance of myelin. Glia. 2000; 29(2):154–165. [PubMed: 10625334]

Sherman LS, Rizvi TA, Karyala S, Ratner N. Cd44 Enhances Neuregulin Signaling by Schwann Cells. The Journal of Cell Biology. 2000; 150(5):1071–1084. [PubMed: 10973996]

Sleeman JP, Arming S, Moll JF, Hekele A, Rudy W, Sherman LS, Kreil G, Ponta H, Herrlich P. Hyaluronate-independent Metastatic Behavior of CD44 Variant-expressing Pancreatic Carcinoma Cells. Cancer Research. 1996; 56(13):3134–3141. [PubMed: 8674073]

Stewart HJS, Rougon G, Dong Z, Dean C, Jessen KR, Mirsky R. TGF-βs upregulate NCAM and L1 expression in cultured Schwann cells, suppress cyclic AMP–induced expression of O4 and galactocerebroside, and are widely expressed in cells of the Schwann cell lineage in vivo. Glia. 1995; 15(4):419–436. [PubMed: 8926036]

Synofzik M, Gonzalez MA, Lourenco CM, Coutelier M, Haack TB, Rebelo A, Hannequin D, Strom TM, Prokisch H, Kernstock C, et al. PNPLA6 mutations cause Boucher-Neuhauser and Gordon

Holmes syndromes as part of a broad neurodegenerative spectrum. Brain. 2014a; 137(Pt 1):69–77. [PubMed: 24355708]

Synofzik M, Kernstock C, Haack TB, Schols L. Ataxia meets chorioretinal dystrophy and hypogonadism: Boucher-Neuhauser syndrome due to PNPLA6 mutations. J Neurol Neurosurg Psychiatry. 2014b

Taveggia C, Zanazzi G, Petrylak A, Yano H, Rosenbluth J, Einheber S, Xu X, Esper RM, Loeb JA, Shrager P, et al. Neuregulin-1 type III determines the ensheathment fate of axons. Neuron. 2005; 47(5):681–694. [PubMed: 16129398]

Topaloglu AK, Lomniczi A, Kretzschmar D, Dissen GA, Kotan LD, McArdle CA, Koc AF, Hamel BC, Guclu M, Papatya ED, et al. Loss-of-function mutations in PNPLA6 encoding neuropathy target esterase underlie pubertal failure and neurological deficits in Gordon Holmes syndrome. J Clin Endocrinol Metab. 2014; 99(10):E2067–E2075. [PubMed: 25033069]

Trapp BD. Myelin-associated glycoprotein. Location and potential functions. Ann N Y Acad Sci. 1990; 605:29–43. [PubMed: 1702602]

Triolo D, Dina G, Lorenzetti I, Malaguti M, Morana P, Del Carro U, Comi G, Messing A, Quattrini A, Previtali SC. Loss of glial fibrillary acidic protein (GFAP) impairs Schwann cell proliferation and delays nerve regeneration after damage. J Cell Sci. 2006; 119(Pt 19):3981–3993. [PubMed: 16988027]

Ushiki T, Ide C. Scanning electron microscopic studies of the myelinated nerve fibres of the mouse sciatic nerve with special reference to the Schwann cell cytoplasmic network external to the myelin sheath. J Neurocytol. 1987; 16(6):737–747. [PubMed: 3450786]

van Tienhoven M, Atkins J, Li Y, Glynn P. Human neuropathy target esterase catalyzes hydrolysis of membrane lipids. J Biol Chem. 2002; 277(23):20942–20948. [PubMed: 11927584]

Velasco M, O'Sullivan C, Sheridan GK. Lysophosphatidic acid receptors (LPARs): Potential targets for the treatment of neuropathic pain. Neuropharmacology. 2016

Wentzell JS, Cassar M, Kretzschmar D. Organophosphate-induced changes in the PKA regulatory function of Swiss Cheese/NTE lead to behavioral deficits and neurodegeneration. PLoS One. 2014; 9(2):e87526. [PubMed: 24558370]

Woodhoo A, Sommer L. Development of the Schwann cell lineage: from the neural crest to the myelinated nerve. Glia. 2008; 56(14):1481–1490. [PubMed: 18803317]

Yu WM, Yu H, Chen ZL, Strickland S. Disruption of laminin in the peripheral nervous system impedes nonmyelinating Schwann cell development and impairs nociceptive sensory function. Glia. 2009; 57(8):850–859. [PubMed: 19053061]

Yuan A, Sasaki T, Kumar A, Peterhoff CM, Rao MV, Liem RK, Julien J-P, Nixon RA. Peripherin Is a Subunit of Peripheral Nerve Neurofilaments: Implications for Differential Vulnerability of CNS and PNS Axons. The Journal of Neuroscience. 2012; 32(25):8501–8508. [PubMed: 22723690]

Zaccheo O, Dinsdale D, Meacock PA, Glynn P. Neuropathy target esterase and its yeast homologue degrade phosphatidylcholine to glycerophosphocholine in living cells. J Biol Chem. 2004

Main points

- NTE/PNPLA6 is expressed in Schwann cells in the sciatic nerve after the pro-myelin stage, and highly expressed in non-myelinating Schwann cells
- NTE/PNPLA6 expression is upregulated after axonal injury
- Loss of NTE/PNPLA6 causes incomplete glial ensheathment of Remak fibers

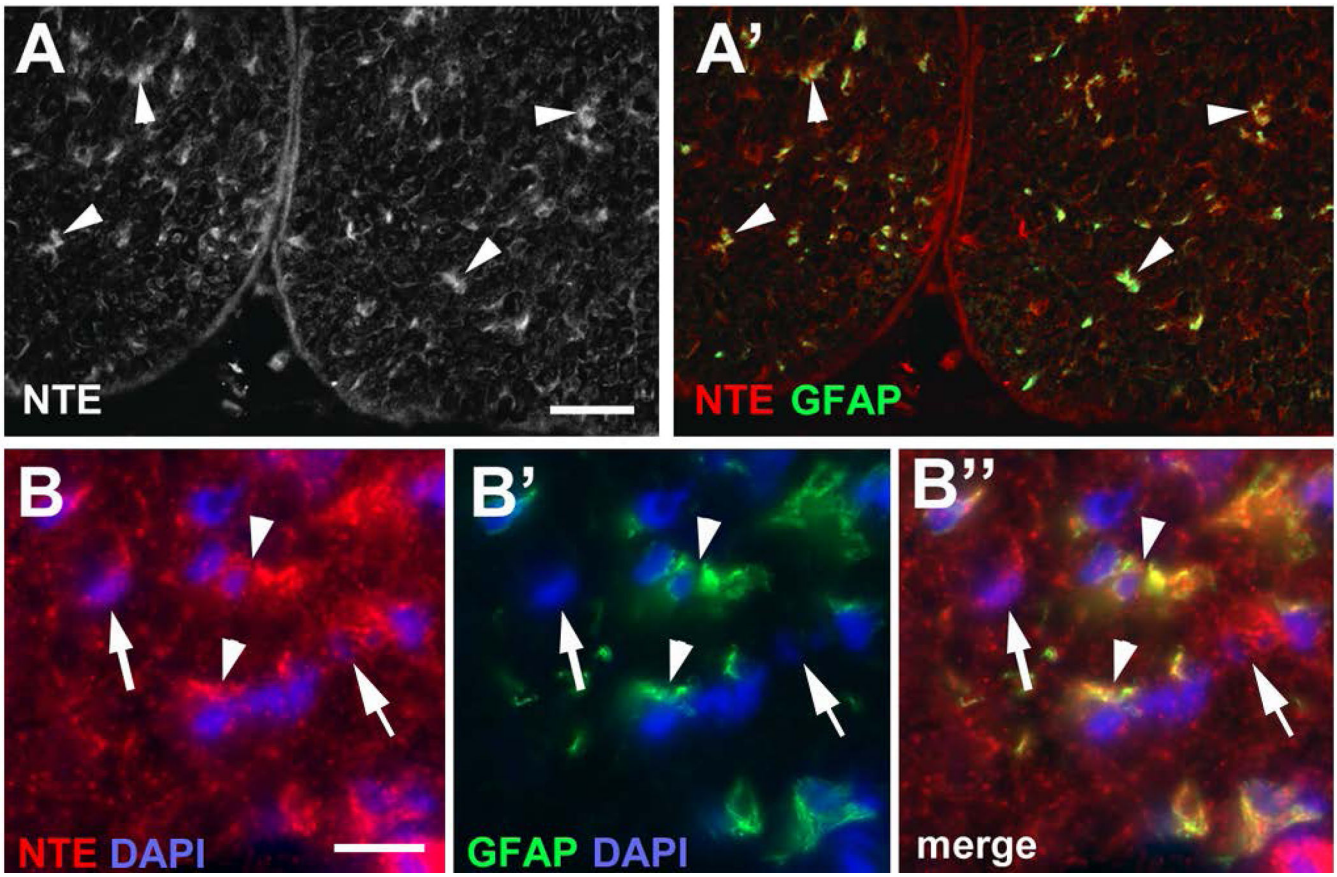

Figure 1.

NTE is detectable in glia in the adult (PND42) sciatic nerve. (A) Using anti-NTE, immunopositive staining is found in the sciatic nerve (arrowheads) and co-localizes with GFAP (A'). (B-B") NTE is detectable in the cell cytoplasm of GFAP-positive cells (arrowheads) and in some non-GFAP positive cells (arrows). NTE is shown in red, GFAP in green, and DAPI in blue. Scale bar in A=30 μm, in B=10 μm.

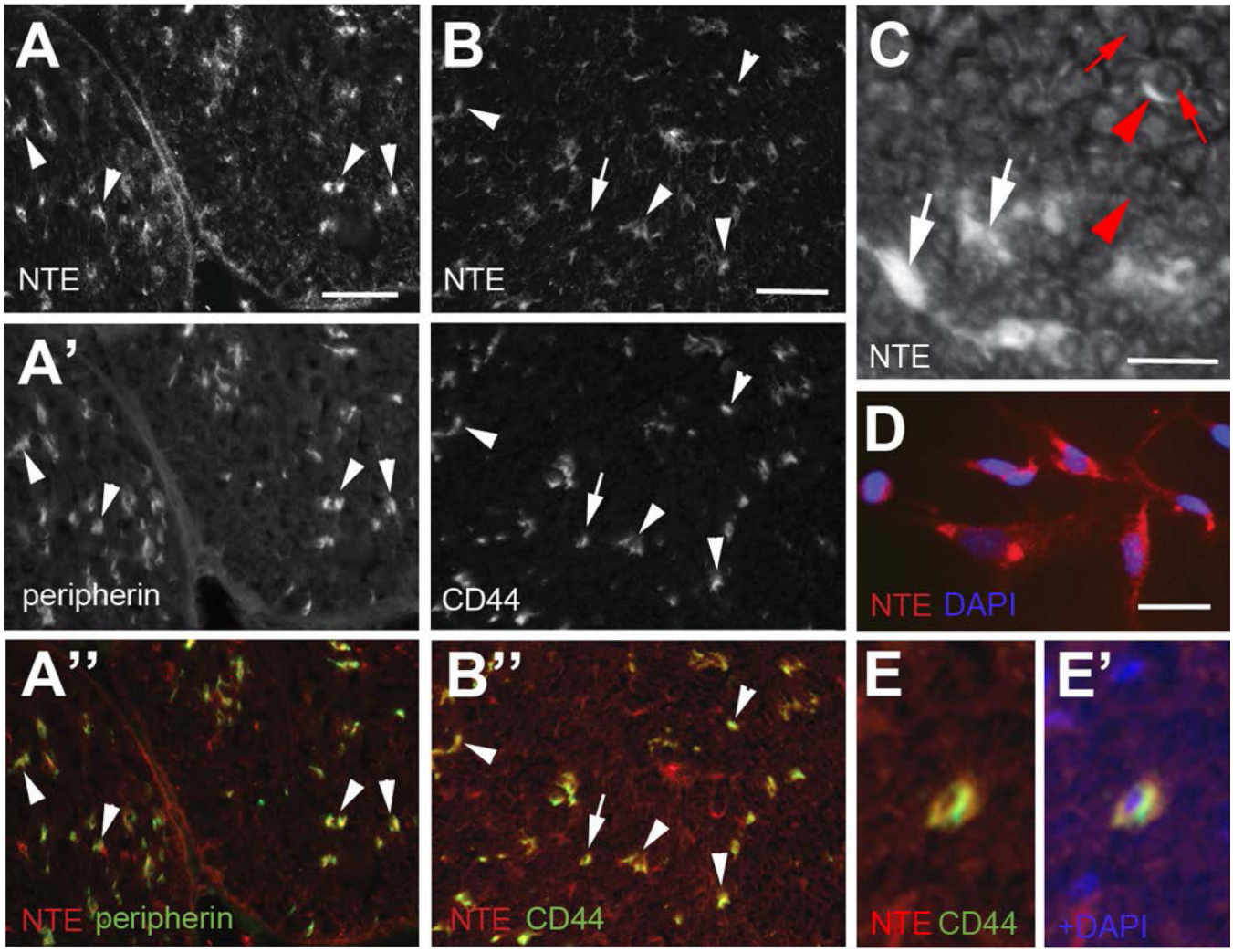

Figure 2.

NTE is highly expressed in non-myelinating Schwann cells. (A-A") NTE is found in close proximity to peripherin (arrowheads), a marker for unmyelinated axons. (B-B") NTE also co-localizes with CD44, which is expressed in adult non-myelinating Schwann cells. (C) In tibial nerve sections, strong staining is found in non-myelinating Schwann cells (white arrows) while weaker staining can be detected in axons (red arrows) and in the cytoplasm of myelinating Schwann cells (red arrowheads). (D) NTE is expressed in cultured Schwann cells. (E, E') Higher magnification view showing co-localization of NTE and CD44 in the neuron labeled with an arrow in B. NTE is shown in red, peripherin and CD44 in green and DAPI in blue. Sections were derived from mice at PND42. Scale bar in A, B=50 μm, in C, D=10 μm.

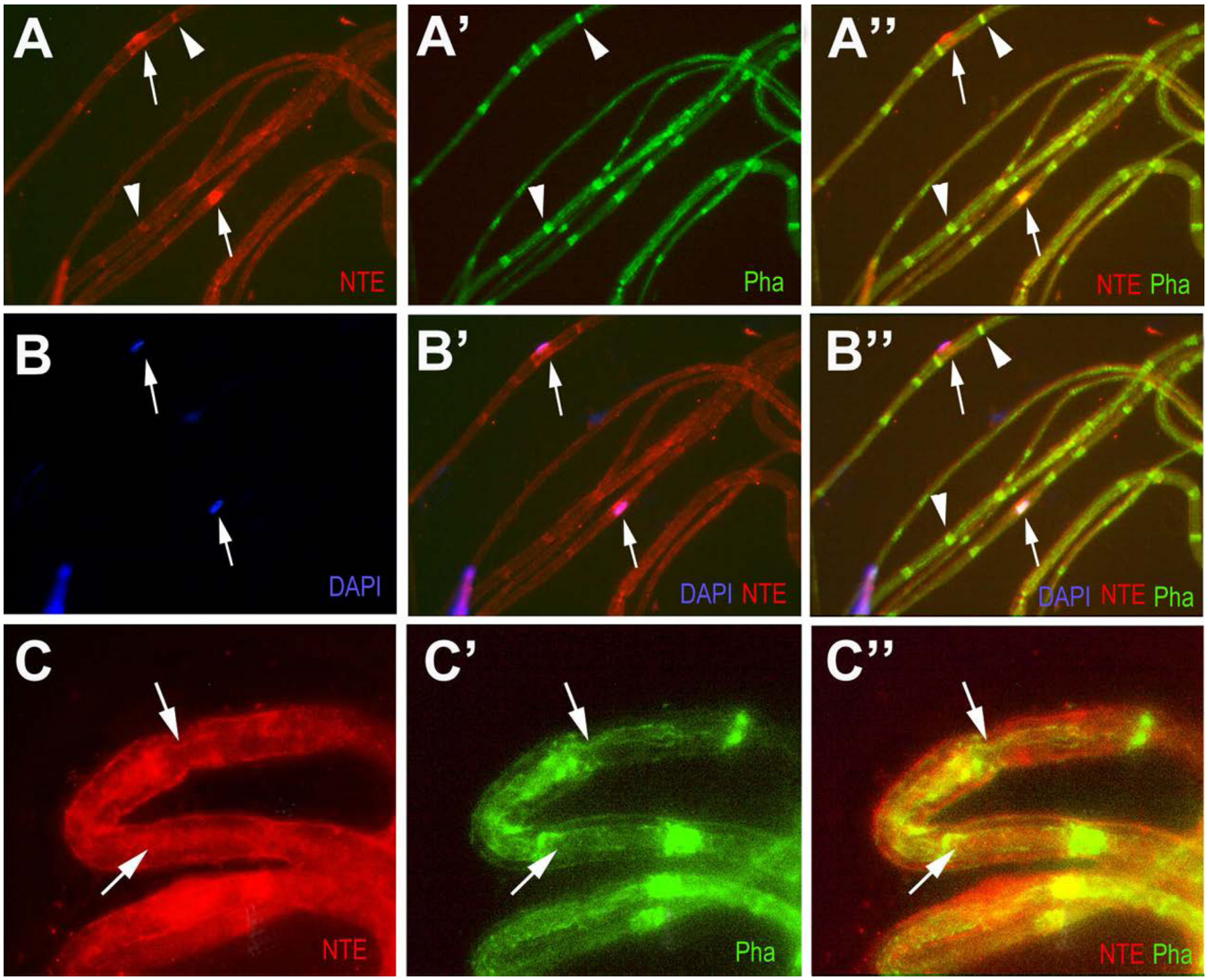

Figure 3.

NTE is enriched in Schmidt-Lanterman incisures and around the nucleus. (A-A") NTE co-localizes with Phalloidin (Pha) in Schmidt-Lanterman incisures (arrowheads). (B-B") Higher levels of NTE can also be found adjacent to nuclei labeled by DAPI (arrows). (C-C") Higher magnification view showing co-localization of NTE and Phalloidin in Cajal bands (arrows). NTE in red, Phalloidin in green and DAPI in blue. Teased fibers were obtained at PND42.

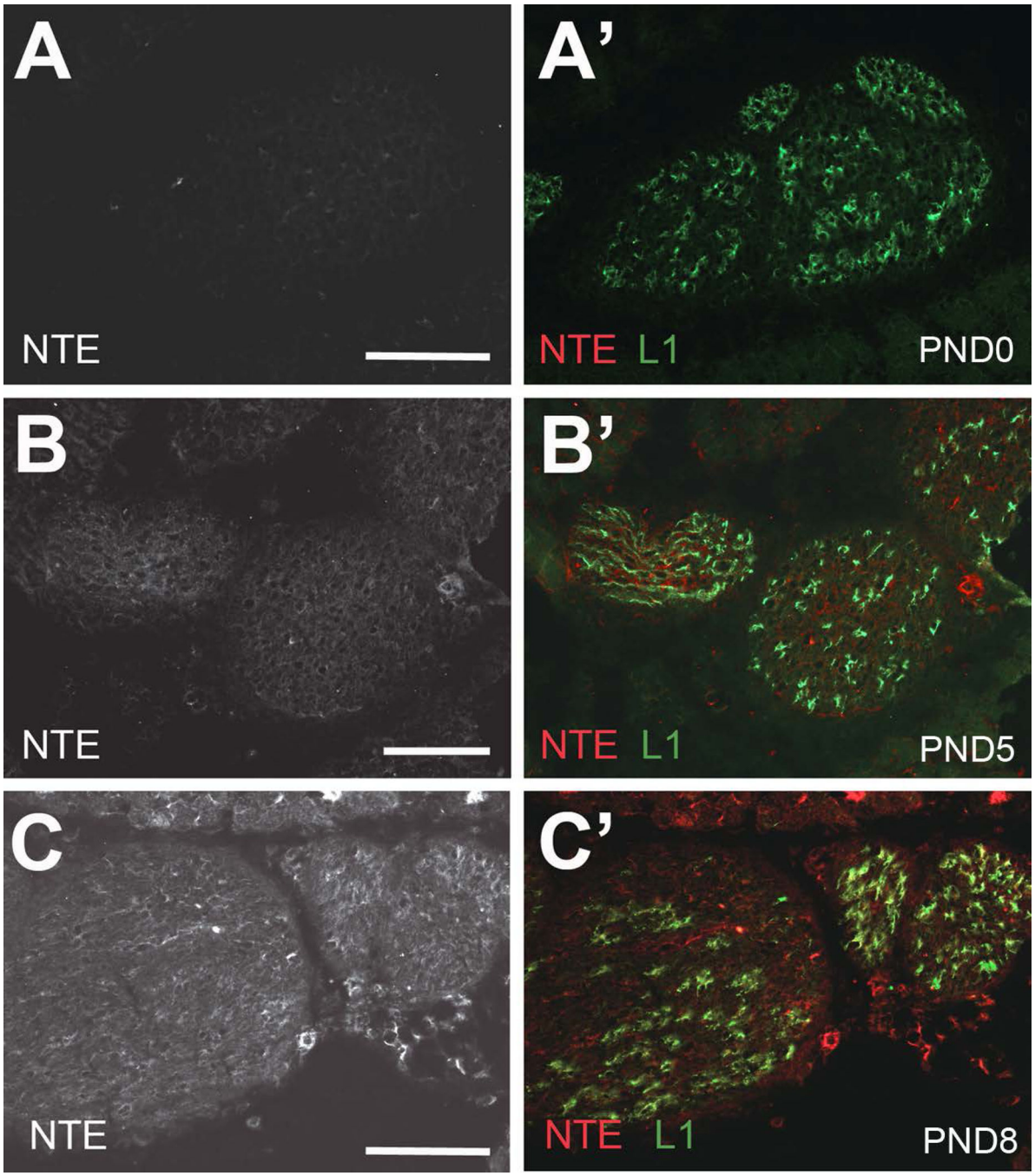

Figure 4.

Developmental expression pattern of NTE. (A, A') At PND0, NTE is not detectable in the sciatic nerve. (B, B') NTE is first apparent at PND5 and its level increase with further aging (C, C', PND8), whereas L1 is detectable at all ages. L1 in green, NTE in red. Scale bar=100 μm.

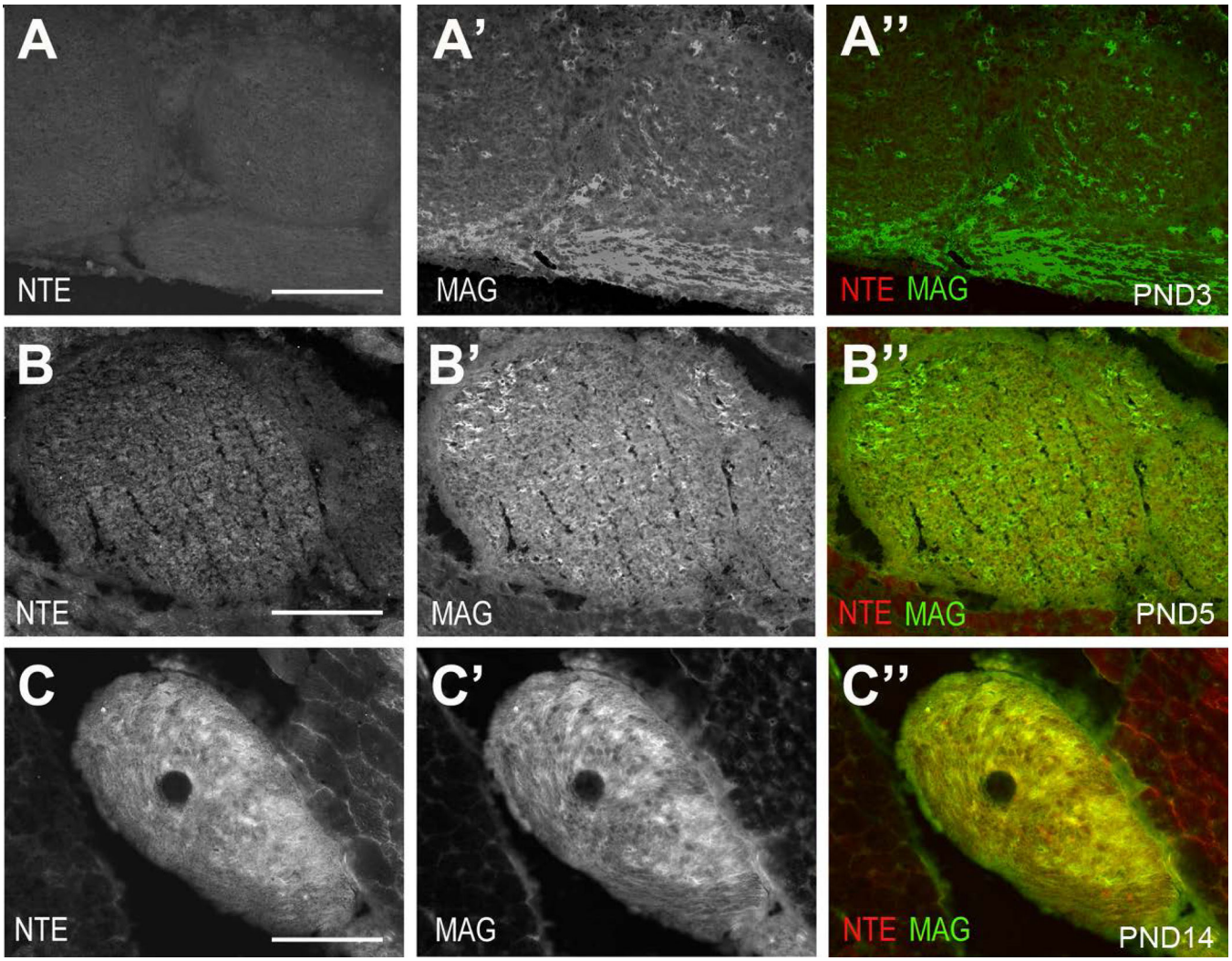

Figure 5.

NTE is not expressed in immature or promyelinating Schwann cells. (A-A") At PND0, some cells are MAG-positive in the sciatic nerve whereas NTE is not detectable. NTE is detectable at PND5 (B-B") and PND14 (C-C"), together with MAG. MAG in green, NTE in red. Scale bar=100,μm.

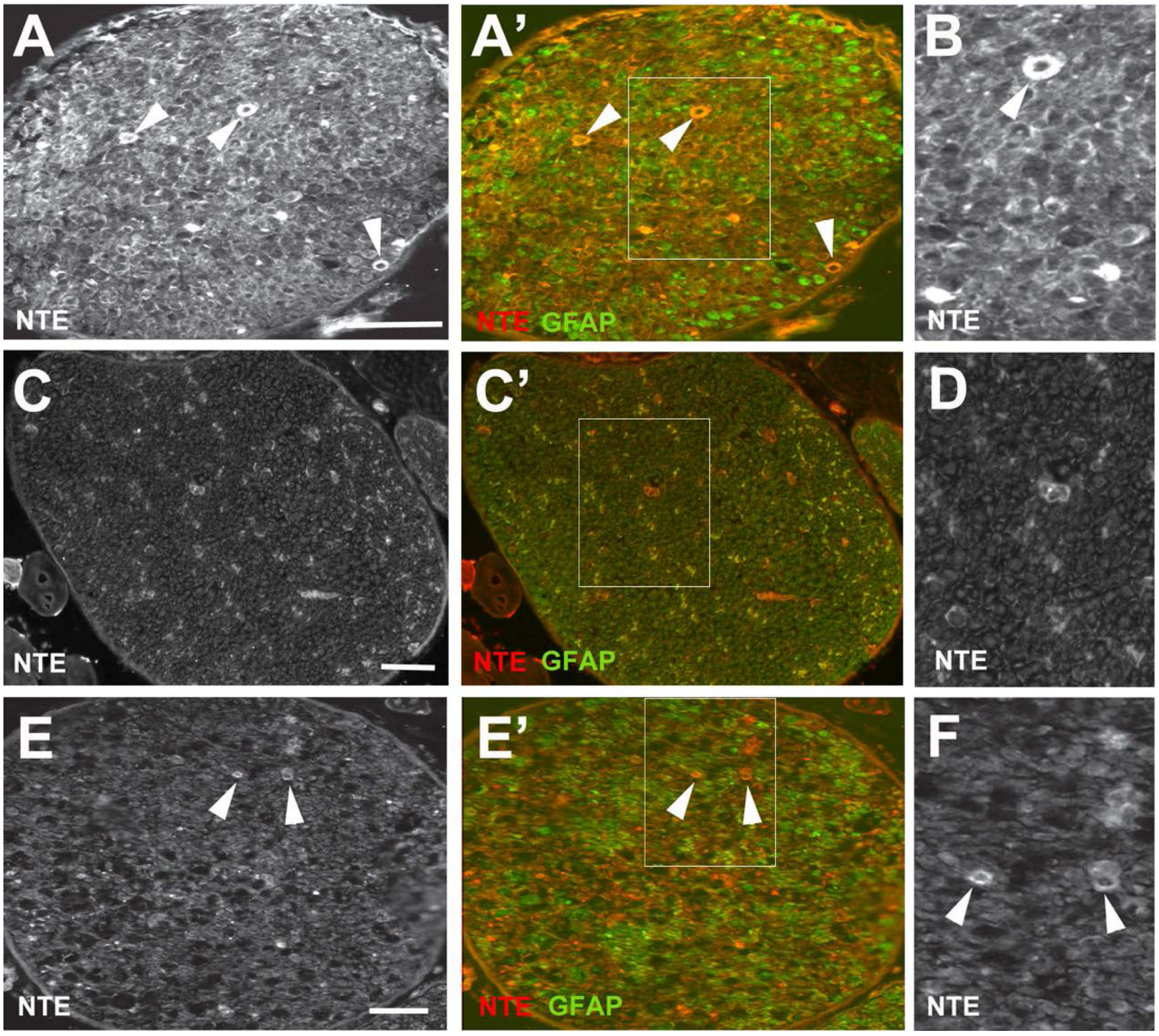

Figure 6.

NTE is upregulated after axotomy. (A, A') 4d after nerve crush, NTE levels are increased in the nerve with strong staining detectable in some ring-shaped structures (arrowheads). (B) Magnified view of the boxed region in A'. (C, C') NTE staining in the uninjured sciatic nerve 4d after nerve crush. (D) Magnified view of the boxed region in C'. (E, E') 11d after nerve injury, an increase in NTE levels is still detectable, including in the ring shaped structures (arrowheads) but the NTE levels have decreased compared to 4d post-injury. (F) Magnified view of the boxed region in E'.NTE in red, GFAP in green. The nerve crush was performed at PND28. Scale bar=50 μm.

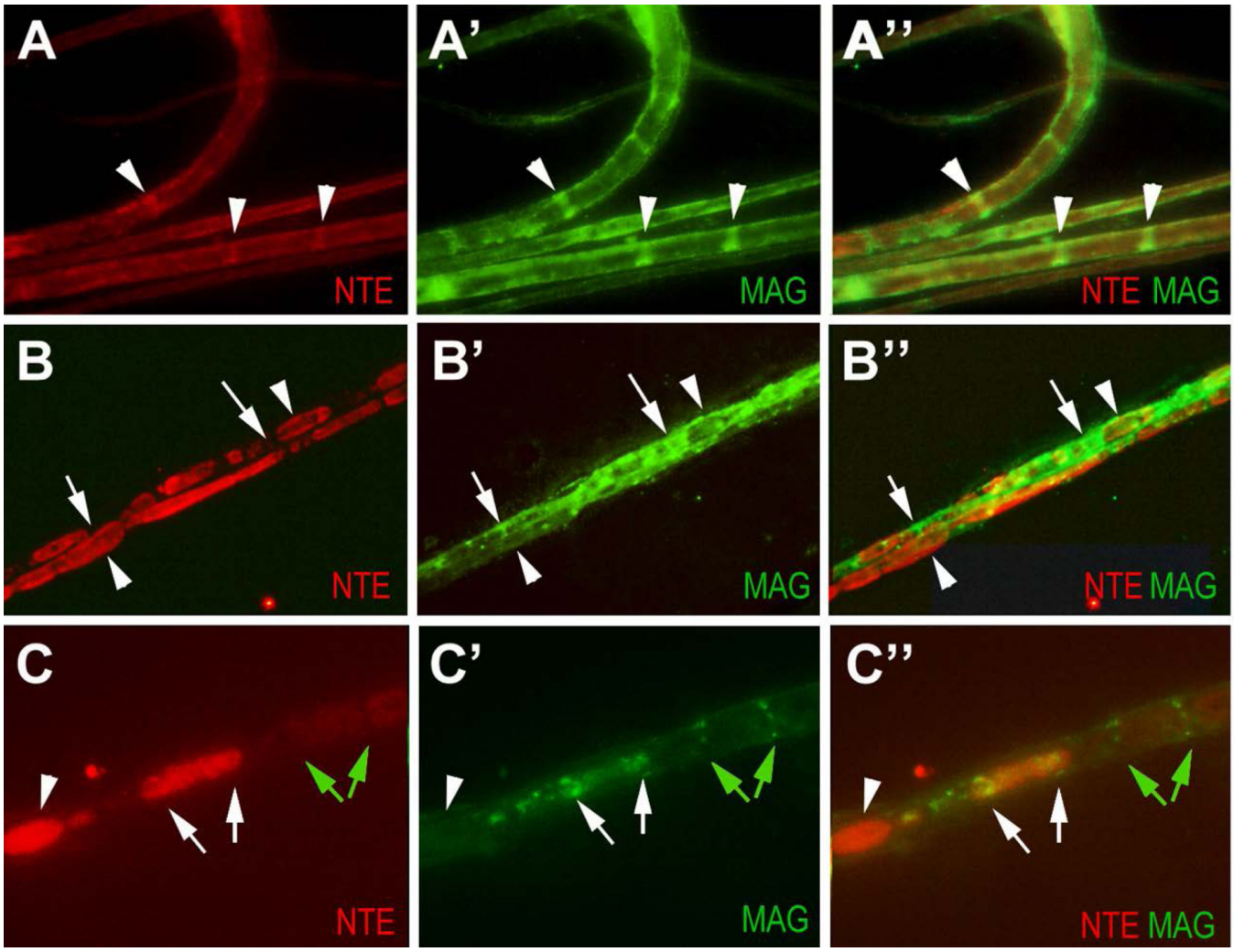

Figure 7.

NTE staining is found in ovoids along the nerve after injury. (A-A") NTE is enriched in Schmidt-Lanterman incisures (arrowheads), co-localizing with MAG in the uninjured nerve. (B-B"). On the crushed side, strong NTE staining is detectable in ovoids along the nerve (arrowheads). NTE staining only co-localize with MAG (arrows) at the margins of ovoids. (C-C") Magnification showing that MAG-positive incisures are adjacent to weakly stained NTE-positive ovoids (green arrows). Another ovoid that contains higher levels of NTE shows MAG-positive staining at the distal and proximal end of the ovoid (white arrows). The ovoid with the highest levels of NTE does not co-stain for MAG, nor is it delimited by MAG staining (arrowhead). The crush was performed at PND42. NTE in red, MAG in green.

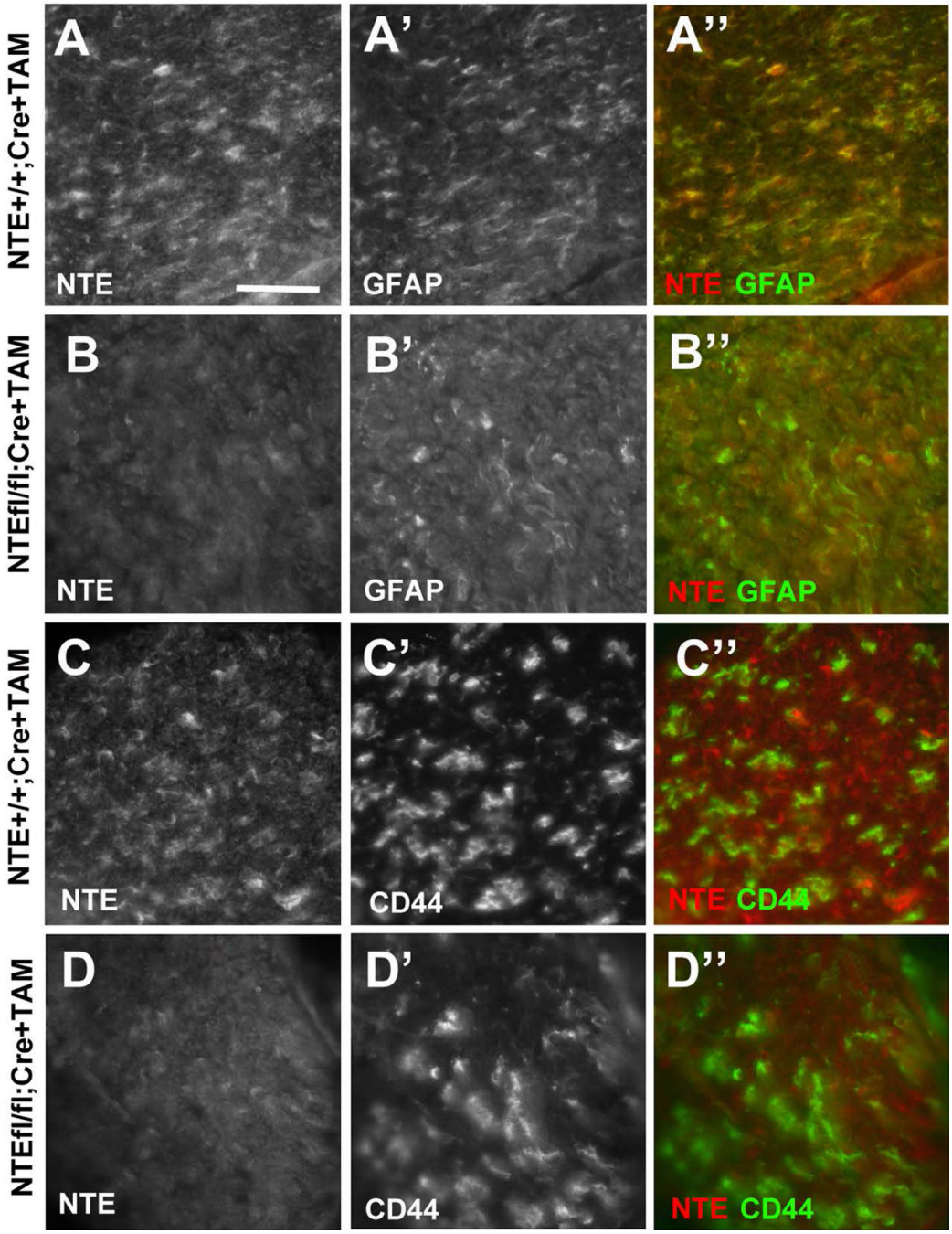

Figure 8.

The conditional knock-out reduces NTE levels. NTE levels are reduced in sciatic nerves of NTE(fl/fl);Cre+ mice (B, D) compared to their NTE(+/+);Cre+ siblings (A, C). The levels of the Schwann cell markers GFAP (A, B) and CD44 (C, D) are not affected by the conditional NTE knock-out. Sections were obtained at PND14. All animals were treated with TAM. NTE in red, GFAP and CD44 in green. Scale bar=30μm.

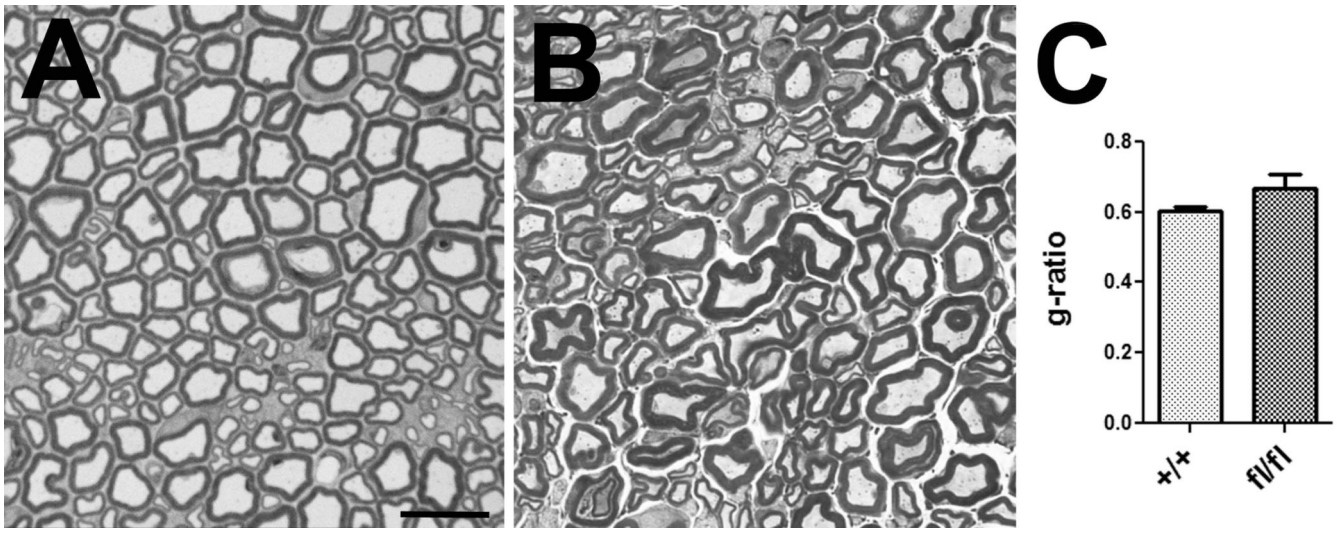

Figure 9.

Glial loss of NTE does not affect myelination. Toluidine-blue stained sciatic nerve sections from TAM treated NTE(+/+);Cre+ (A) and NTE(fl/fl);Cre+ mice (B). (C) Determining the g-ratio did not reveal a significant difference between the conditional knock-out animals and controls. Two mice were used per genotype. 200 axons from each genotype were analysed in C. Histogram represents means ± SEM. Scale bar=5μm.

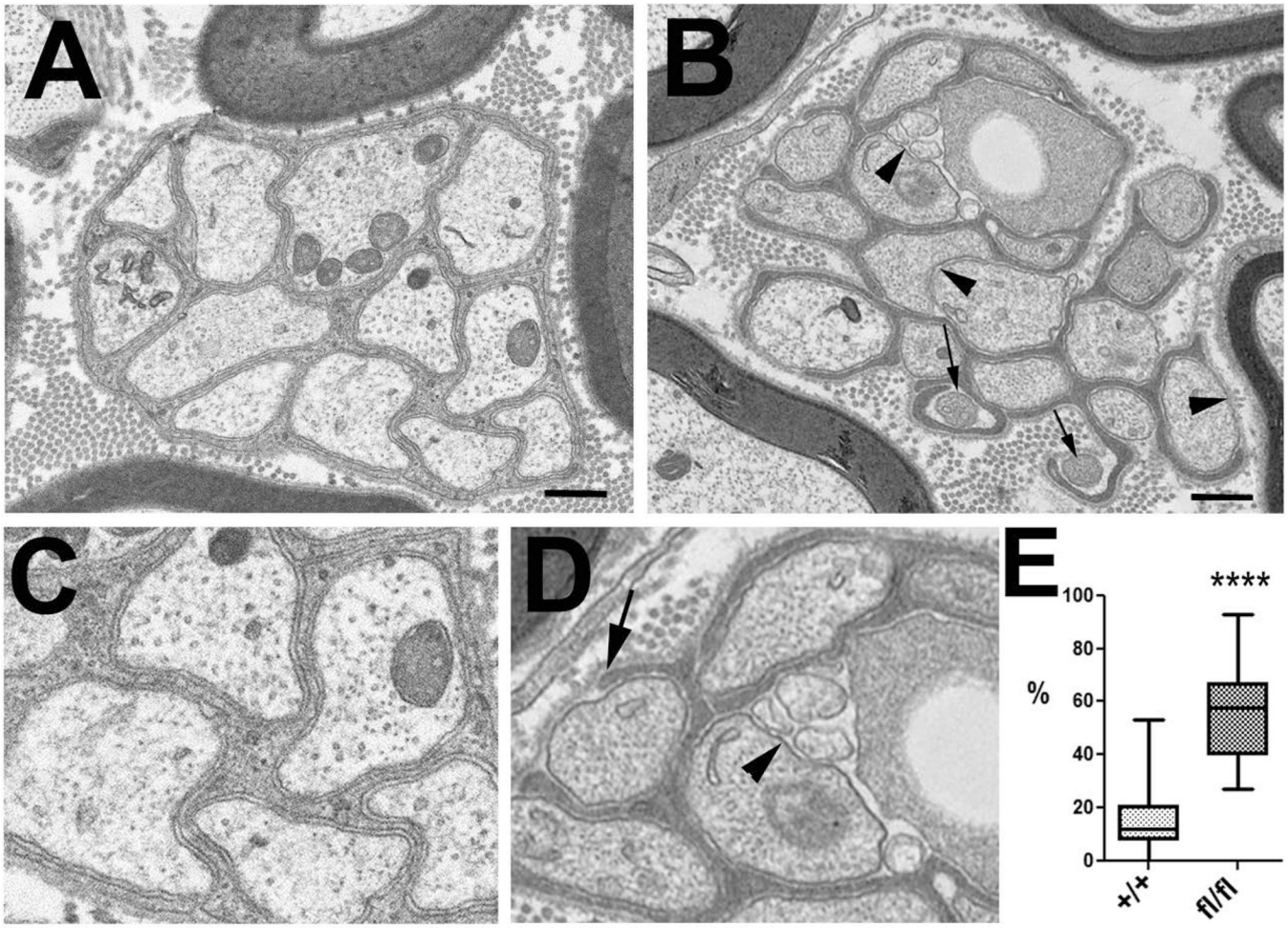

Figure 10.

The conditional NTE knock-out results in incomplete glial wrapping of Remak fibers. (A, C) Electron microscopic image from a Remak bundle in a TAM treated NTE(+/+);Cre+ mouse. (B, D) Remak bundle in a TAM-treated NTE(fl/fl);Cre+ mouse. The arrowheads point to areas where the glial sheath is missing, arrows point to electron dense, shrunken axons. (D) Quantification showing the percentage of axons in a Remak bundle that are not completely wrapped by glia. The horizontal line represents the medians, boxes denote the 25% and 75% quartiles, and whiskers express 10% and 90% quantiles. Twenty Remak bundles were analyzed per genotype, with two mice used for each experiment. Scale bar=500 nm. ***$p < 0.0001$ (Student's t-test).